International Journal of Mass Spectrometry 273 (2008) 145–150

Contents lists available at ScienceDirect

International Journal of Mass Spectrometry

journal homepage: www.elsevier.com/locate/ijms

Electron impact calculations of total and ionization cross-sections for Germanium Hydrides (GeH_X; $X = 1–4$) and Digermane, Ge_2H_6

Minaxi Vinodkumar[a,*], Chetan Limbachiya[b], Kirti Korot[a], K.N. Joshipura[c], Nigel Mason[d]

[a] V.P. & R.P.T.P. Science College, Vallabh Vidyanagar 388 120, Gujarat, India
[b] P.S. Science College, Kadi 382 715, Gujarat, India
[c] Department of Physics, Sardar Patel University, Vallabh Vidyanagar, Gujarat, India
[d] Department of Physics & Astronomy, Open University, Milton Keynes MK7 6AA, UK

ARTICLE INFO

Article history:
Received 15 February 2008
Received in revised form 1 April 2008
Accepted 1 April 2008
Available online 8 April 2008

PACS:
34.80 Bm

Keywords:
Ionization cross-sections
Germane
SCOP

ABSTRACT

In this article we report calculations of the total elastic Q_{el}, total ionization, Q_{ion}, and total (complete), Q_T, cross-sections for the germanium hydrides GeH_X ($X = 1–4$) and digermane (Ge_2H_6) upon electron impact for energies from circa threshold to 2000 eV. Spherical Complex Optical Potential (SCOP) formalism is employed to evaluate Q_{el}, Q_{inel} and Q_T. Total ionization cross-sections, Q_{ion}, are derived from the total inelastic cross-sections, Q_{inel}, using a semi-empirical formulation developed by us called 'Complex Spherical Potential-ionization contribution' (CSP-ic) method. A comparison of the various cross-sections is provided to show their relative contribution to the total cross-section Q_T. Present results are compared with available experimental and theoretical data wherever possible and overall agreement is good. However, no experimental data on the Q_{ion} are available for the germanium hydrides, GeH_X, $X = 1–3$ or digermane.

1. Introduction

Germanium is an important semiconductor element. Germanium hydrides, in particular germane, GeH_4, and digermane, Ge_2H_6, are widely used as feed gases in plasma deposition and doping processes in the semiconductor industries. GeH_X ($X = 1–3$) radicals are readily formed in a GeH_4 plasma and control both the physical and chemical properties of the resultant plasma. Hence the ionization properties of all these hydrides are important quantities in order to understand and model low-temperature GeH_4 plasmas [1]. However, despite their industrial and environmental importance, studies of electron interactions with these molecules remain scarce. Indeed, total ionization cross-sections are only available through theoretical studies while there is paucity of experimental data for all these species except for germane [2]. This is in contrast to other group IV tetra hydrides (such as CH_4 and SiH_4), which are extensively investigated in the field of electron-molecule collisions.

More generally electron impact ionization cross-sections of molecules and radicals are important quantities in a variety of applications such as low-temperature processing plasmas, fusion edge plasmas, gas discharges, planetary, stellar and cometary atmospheres, radiation chemistry, mass spectrometry and chemical analysis. Rigorous quantum mechanical calculations of ionization cross-sections for molecular targets are beyond the scope of current quantum-mechanical electron collision theory for essentially all molecules. Hence a variety of approximate methods (often semi-classical) have been developed to generate ionization cross-sections for input into modeling codes for various applications such as fusion edge plasma and plasma processing. Examples include the Binary Encounter Bethe, BEB method by Ali et al. [3] and the Deustch and Märk (DM) formalism reviewed by Probst et al. [1] while Szmytkowski and Denga [4] have reported estimated ionization cross-sections from threshold to 250 eV using a simple regression formula.

In the present paper we report total ionization cross-sections for all the listed targets from threshold to 2 keV calculated using the semi-empirical method, CSP-ic developed by us. Also we have calculated total elastic, Q_{el}, and total (complete), cross-sections, Q_T for all these targets. The total cross-sections, TCS (including elastic as well as all energetically possible inelastic channels) serve as an upper limit to the theoretical as well experimental cross-sections as they include all the elastic and inelastic processes occurring during the collision process. Here we are interested in the intermediate and high-energy region (from ionization threshold up to 2 keV) where almost all inelastic channels (rotational, vibrational,

* Corresponding author.
E-mail address: minaxivinod@yahoo.co.in (M. Vinodkumar).

1387-3806/$ – see front matter © 2008 Elsevier B.V. All rights reserved.
doi:10.1016/j.ijms.2008.04.001

electronic excitation, ionization, dissociation processes, etc.) are open [5].

Previous work is largely limited to germane. Dillon et al. [6] have reported total elastic and total inelastic cross-sections for germane for incident energies between 1 and 100 eV. Winsted et al. [7] have reported DCS and integral elastic cross-sections for incident energies from 5 to 30 eV and Baluja et al. [8] have reported total cross-sections in the range 10–1000 eV. Lee et al. [2] have reported integral elastic cross-sections for low impact energies ranging from 0.2 to 100 eV. The total cross-section has been reported by two groups viz. Mozejko et al. [9] for low incident energies from 0.5 to 250 eV and Karwasz [10] for intermediate to high incident energies from 75 to 4000 eV.

In the next section we will describe the theoretical formalism employed to calculate total elastic, total ionization and total (complete) cross-sections for these targets.

2. Theoretical methodology

Details of the theoretical formalism employed here to determine total cross-sections (TCS) for the impact of electrons can be found in our earlier papers [5,11–17] so only a brief summary will be given here. We have employed the well-known spherical complex optical potential (SCOP) formalism, through which the total elastic cross-sections, Q_{el}, and its inelastic counterpart, Q_{inel}, are obtained such that:

$$Q_T(E_i) = Q_{el}(E_i) + Q_{inel}(E_i) \quad (1)$$

In the present range of electron energy (threshold to 2 keV), many scattering channels are open leading to discrete as well as continuum transitions in the target. Therefore we represent the electron-molecule system by a complex potential:

$$V(r, E_i) = V_R(r, E_i) + i\,V_I(r, E_i) \quad (2)$$

such that

$$V_R(r, E_i) = V_{st}(r) + V_{ex}(r, E_i) + V_{pol}(r, E_i) \quad (3)$$

The three terms on the RHS of Eq. (3) represent various real potentials arising from the electron target interactions namely, static, exchange and the polarization potentials, respectively. The most important basic input for evaluating all these potentials is the charge density of the target. This is obtained from the spherically averaged molecular charge density $\rho(r)$, which is determined from the constituent atomic charge densities derived from the wave functions of Bunge and Barrientos [18]. For germanium hydride molecule the total charge density is made single centered by expanding the charge density of lighter hydrogen atom at the centre of heavier germanium atom. In the case of the Ge_2H_6 molecule, we have used a group additivity rule and identified two scattering centers as lying about the two germanium atoms. The molecular charge density, $\rho(r)$, so obtained is renormalized to incorporate the covalent bonding [12]. For the exchange potential, we have employed Hara's 'free electron gas exchange model' [19] which is parameter free and energy dependent. For the polarization potential V_p, we have used a parameter free model of correlation—the polarization potential given by Zhang et al. [20] which contains some multipole non-adiabatic corrections in the intermediate region and it smoothly approaches the correct asymptotic form at large 'r'.

Finally, the imaginary part V_I of the complex potential is the absorption potential which represents appropriately the combined effects of all inelastic channels. Here, we employed a well-known non-empirical quasi-free model form given by Staszeweska et al. [21], thus,

$$V_{abs}(r, E_i) = -\rho(r)\sqrt{\frac{T_{loc}}{2}}\left(\frac{8\pi}{10k_F^3E_i}\right) \times \theta(p^2 - k_F^2 - 2\Delta) \times (A_1 + A_2 + A_3) \quad (4)$$

The local kinetic energy of the incident electron is

$$T_{loc} = E_i - (V_{st} + V_{ex}) \quad (5)$$

The absorption potential is not sensitive to long range potentials like V_{pol}. In Eq. (4), $p^2 = 2E_i$, $kF = [3\pi^2\theta(x)]^{1/3}$ is the Fermi wave vector and Δ is an energy parameter. Further $\theta(x)$ is the Heaviside unit step-function, such that $\theta(x) = 1$ for $x \geq 0$, and is zero otherwise. The dynamic functions A_1, A_2 and A_3 occurring in the Eq. (4) depend differently on $\theta(x)$, I, Δ and E_i. The energy parameter Δ determines a threshold below which $V_{abs} = 0$, and the ionization or excitation is prevented energetically. In fact Δ is the governing factor which decides the values of total inelastic cross-section and that is one of the characteristics of Staszewska model [21]. We have modified the original model by considering Δ as a slowly varying function of E_i around I. The justification for the same is discussed by Vinodkumar et al. [11,12] and Joshipura et al. [15,17]. Briefly, a preliminary calculation for Q_{inel} is done with a fixed value $\Delta = I$. From this the value of incident energy at which our Q_{inel} reaches its peak, named as E_p is obtained. Further, Δ as a variable accounts for the screening of the absorption potential in the target charge-cloud region, Blanco and Garcia [22]. This is meaningful since Δ fixed at I would not even allow excitation at incident energy $E_i \leq I$. On the other hand, if the parameter Δ is much less than the ionization threshold, then V_{abs} becomes unduly high near the peak position. The modification introduced in our paper has been to assign a reasonable minimum value $0.8\,I$ to Δ and express this parameter as a function of E_i around I as follows:

$$\Delta(E_i) = 0.8I + \beta(E_i - I) \quad (6)$$

In Eq. (6) β is then obtained by requiring that $\Delta = I + 1$ (eV) at $E_i = E_p$, beyond which Δ is held constant and equal to I. The expression for $\Delta(E_i)$, Eq. (6), is meaningful since Δ fixed at I would not allow excitation at incident energies $E_i \leq I$. On the other hand, if parameter Δ is much less than the ionization threshold, then V_{abs} becomes substantially high near the peak position. In view of Eq. (6) the present method becomes semi-empirical. After generating the full complex potential given in Eq. (2), we solve the Schrödinger equation numerically using partial wave analysis to obtain complex phase shifts that are then used to find cross-sections given in Eq. (1).

The total inelastic cross-section, Q_{inel}, cannot be measured directly. However, experimentally the total inelastic cross-sections can be obtained as the difference between experimental values of grand total cross-sections (beam attenuation experiments) and purely elastic cross-sections (obtained by integrating differential elastic cross-sections). In practice very few experimental groups are doing both the measurements simultaneously, and different groups work in different energy regimes and their experimental uncertainty is also different and hence there is difficulty in obtaining total inelastic cross-sections from the experiment.

In fact the measurable quantity which is of more practical importance is the total ionization cross-section, Q_{ion}. Q_{inel} can be partitioned into two main contributions viz.:

$$Q_{inel}(E_i) = \sum Q_{exc}(E_i) + Q_{ion}(E_i) \quad (7)$$

where the first term is the sum over total excitation cross-sections for all accessible electronic transitions. The second term is the total cross-sections of all allowed ionization processes induced by the

incident electrons. The first term arises mainly from the low-lying dipole allowed transitions for which the contribution of excitation cross-sections to Q_{inel}, progressively decreases compared to the ionization cross-sections with increase of energy. This is because the peak of excitation cross-sections occurs at lower energies hence while the Q_{ion} is rising in the intermediate region $\sum Q_{exc}$ is falling. The Q_{ion} in Eq. (7) for electron impact ionization corresponds to continuum as against discrete optically allowed electronic excitation channels. Therefore typically over 100 eV or so, ionization dominates over excitation.

Thus from Eq. (7):

$$Q_{inel}(E_i) \geq Q_{ion}(E_i) \tag{8}$$

Now, in order to extract Q_{ion} from Q_{inel}, a reasonable approximation can be evoked by using a ratio function:

$$R(E_i) = \frac{Q_{ion}(E_i)}{Q_{inel}(E_i)} \tag{9}$$

such that, $0 < R \lesssim 1$.

$R = 0$ when $E_i \leq I$. For a number of stable atoms and molecules like Ne, O_2, H_2O, CH_4, SiH_4 etc., for which the experimental cross-sections Q_{ion} are known accurately [23–25] the ratio R rises steadily as the energy increases above the threshold, and approaches unity at high energies. Thus,

$$\begin{aligned} R(E_i) &= 0 \quad \text{for} \quad E_i \leq I \\ &= R_P \quad \text{at} \quad E_i = E_P \\ &\cong 1 \quad \text{for} \quad E_i \gg E_P \end{aligned} \tag{10}$$

where 'E_p' stands for the incident energy at which the calculated Q_{inel} attains its maximum value. R_p is the value of R at $E_i = E_p$. Perhaps the first ever estimate of ionization in relation to excitation processes was made by Turner et al. [26]. They concluded from semi-empirical calculations that in gaseous water (H_2O), ionization was more probable than excitation above ~30 eV. If σ_{ion} and σ_{exc} are the cross-sections of ionization and excitation, respectively, then almost above 100 eV:

$$\frac{\sigma_{ion}}{\sigma_{ion} + \sigma_{exc}} \approx 0.75 \tag{11}$$

It should be noted here that the denominator in Eq. (11) represents the total inelastic cross-sections. Hence this ratio is similar to the ratio defined by the authors vide Eq. (9). The general observation is that, at energies close to peak of ionization, the contribution of Q_{ion} is about 70–80% of the total inelastic cross-sections Q_{inel}. This behavior is attributed to the smaller values of $\sum Q_{exc}$ compared to Q_{ion} with the increase in energy beyond E_p value. The ionization threshold for the targets studied here is less than 13 eV hence we have chosen lower limit, i.e. $R_p \approx 0.7$. Here the choice of this value of R_p is approximate but physically justified. The peak position E_p (typically around 50 eV) occurs at an incident energy where the discrete excitation cross-sections are on the wane, while the ionization cross-sections are rising, suggesting that R_p value should be above 0.5 but still below 1. However the choice of R_p in Eq. (10) is not rigorous and introduces uncertainty in the final results [17]. We note that in view of the approximations made here, no definitive values are claimed, but by and large our results fall within the experimental error limits in most of the cases. It has been by now tested for large number of atoms and molecules and it is observed that the proposed uncertainty is found to be 10–15% [5,11–17]. Compared to the uncertainty in the Q_{ion}, the uncertainty in $\sum Q_{exc}$ cross-sections would be larger. For calculating the Q_{ion} from Q_{inel} we need R as a continuous function of energy for $E_i > I$; hence we represent the ratio R in the following manner:

$$R(E_i) = 1 - f(U) \tag{12}$$

Presently the above ratio has been determined using the following analytical form [5,11–17].

$$R(E_i) = 1 - C_1 \left(\frac{C_2}{U + a} + \frac{\ln(U)}{U} \right) \tag{13}$$

where U is the dimensionless variable defined by,

$$U = \frac{E_i}{I}$$

The reason for adopting a particular functional form of $f(U)$ in Eq. (13) can be understood as follows. As E_i increases above I, the ratio R increases and approaches 1, since the ionization contribution rises and the discrete excitation term in Eq. (7) decreases. The discrete excitation cross-sections, dominated by dipole transitions, falls off as their contribution decreases at higher energies, while the contribution of total ionization cross-sections increases as energy increases beyond ionization threshold. Accordingly the decrease of the function $f(U)$ must also be proportional to $\ln(U)/U$ in the high range of energy. However, the two-term representation of $f(U)$ given in Eq. (13) is more appropriate since the first term in the brackets ensures a better energy dependence at low and intermediate energy, E_i and the second term governs the situation at high energies. The dimensionless parameters C_1, C_2, and a, involved in Eq. (13) reflect the properties of the target under investigation. The three conditions stated in Eq. (10) are used to determine these three parameters and hence the Ratio R. This method is called the complex scattering potential-ionization contribution (CSP-ic). This method has been tested for varieties of targets [5,11–17]. Having obtained Q_{ion} through CSP-ic, the summed excitations cross-sections $\sum Q_{exc}$ can be easily calculated using Eq. (7). However the values of $\sum Q_{exc}$ for all these targets are not reported here but are available with the authors.

3. Results

The theoretical approach of SCOP along with our CSP-ic method discussed above allows us to determine the total cross-sections Q_T, Q_{el} and Q_{ion} along with a useful estimate on electronic excitations in terms of the summed cross-section $\sum Q_{exc}$. The present results for the total ionization cross-sections, total elastic and total (complete) cross-sections and for germanium hydrides and digermane are presented in Table 1 and are also plotted in Figs. 1–7. Total ionization cross-sections are calculated using the CSP-ic method. For germane in Fig. 5, we have plotted total elastic and total (complete) cross-sections in addition to total ionization cross-section. Fig. 8 presents a bar chart illustrating the relative contribution of various total cross-sections to the total cross-section for germane at $E_i = 80$ eV.

Fig. 1 compares the total ionization cross-section for e-GeH scattering with available data. Since there are no experimental data to compare with our results, they are compared with two previous theoretical evaluations [1,3]. The present results are in very good accord with theoretical values of Ali et al. [3] using the BEB method at low energies and are only slightly higher at the peak value and slightly lower at high energies. The theoretical values of Probst et al. [1], using the DM method, are higher than both the present and BEB theories particularly in the peak region whilst the peak in the cross-section is also predicted to lie at a slightly lower energy. However the shape of the cross-section curve is almost the same for all three theories.

Fig. 2 shows the total ionization cross-sections for electron impact on GeH_2. Once again there are no experimental data in the literature with which to compare but Ali et al. [3] and Probst et al. [1] have made calculations. The present results are in very good agreement with both the theoretical values above 100 eV. Below

Table 1
Total ionization, total elastic and total (complete) cross-sections of germanium hydrides (GeH_X; $X = 1–4$) and digermane (Ge_2H_6)

E_i (eV)	Q_{ion}					Q_{el}					Q_T				
	GeH	GeH_2	GeH_3	GeH_4	Ge_2H_6	GeH	GeH_2	GeH_3	GeH_4	Ge_2H_6	GeH	GeH_2	GeH_3	GeH_4	Ge_2H_6
10	0.5	0.06	0.08	–	–	39.70	41.78	44.49	–	–	40.90	42.43	45.02	–	–
15	2.24	1.16	1.23	1.26	0.57	29.43	32.05	35.30	38.06	66.01	34.11	35.53	37.95	39.86	67.67
20	3.53	2.54	2.68	2.75	2.39	22.37	24.72	27.41	30.98	53.67	29.39	30.63	33.01	34.85	58.54
25	4.37	3.64	3.98	3.67	3.75	17.88	19.52	21.43	25.10	43.73	25.87	27.07	29.09	30.78	51.89
30	4.77	4.21	4.73	4.43	5.37	15.18	16.60	17.70	20.26	35.85	22.99	24.51	26.01	27.44	46.92
35	5.02	4.5	5.08	4.91	6.38	13.13	14.38	15.39	17.07	30.46	20.85	22.56	23.74	24.94	42.84
40	5.16	4.66	5.29	5.19	6.97	11.67	12.76	13.55	15.01	26.89	19.38	20.82	21.93	23.03	39.66
50	5.24	4.81	5.42	5.41	7.49	9.58	10.79	11.44	12.49	22.60	17.06	18.28	19.33	20.37	34.94
60	5.18	4.83	5.44	5.41	7.64	8.44	9.59	9.99	10.93	19.71	15.56	16.53	17.55	18.56	31.82
70	5.07	4.77	5.37	5.31	7.65	7.68	8.68	9.12	9.87	17.75	14.44	15.32	16.22	17.15	29.35
80	4.94	4.68	5.26	5.18	7.56	6.99	7.89	8.27	9.06	16.28	13.55	14.39	15.22	15.98	27.32
90	4.81	4.58	5.15	5.03	7.42	6.66	7.42	7.79	8.41	15.09	12.84	13.55	14.33	14.99	25.61
100	4.68	4.47	5.02	4.88	7.25	6.27	6.95	7.29	7.86	14.11	12.16	12.90	13.70	14.13	24.14
200	3.65	3.56	3.98	3.76	5.74	4.15	4.48	4.71	5.12	9.27	8.49	8.78	9.15	9.46	16.14
300	3.04	2.98	3.31	3.1	4.75	3.30	3.44	3.62	4.00	7.28	6.69	6.92	7.16	7.42	12.74
400	2.63	2.59	2.86	2.67	4.07	2.72	2.83	3.02	3.34	6.09	5.64	5.79	6.01	6.21	10.63
500	2.31	2.28	2.53	2.36	3.56	2.34	2.42	2.62	2.88	5.26	4.88	4.98	5.22	5.38	9.19
600	2.05	2.06	2.27	2.13	3.16	2.09	2.21	2.33	2.54	4.65	4.32	4.43	4.59	4.77	8.12
700	1.85	1.86	2.05	1.94	2.88	1.88	1.99	2.17	2.28	4.19	3.87	3.98	4.17	4.30	7.30
800	1.68	1.7	1.87	1.79	2.64	1.71	1.87	1.96	2.09	3.83	3.52	3.68	3.77	3.94	6.67
900	1.54	1.59	1.7	1.66	2.43	1.57	1.72	1.83	1.93	3.55	3.21	3.41	3.55	3.64	6.15
1000	1.42	1.47	1.59	1.55	2.24	1.48	1.64	1.73	1.80	3.33	2.99	3.19	3.32	3.40	5.71
2000	0.85	0.89	0.93	0.96	1.37	0.98	1.04	1.09	1.15	2.16	1.86	1.97	2.05	2.12	3.59

100 eV our values are slightly higher than those of Ali et al. [3]. The theoretical values of Probst et al. [1] are again higher than the present results and peak at a lower energy.

In Fig. 3 we compare the total ionization cross-sections for e-GeH_3 scattering with available data. No experimental data is found in the literature. The present results are in good accord with the theoretical values of Ali et al. [3] and Probst et al. [1] above 100 eV. While at energies below 100 eV the present data falls in between the theoretical data of Ali et al. [3] and Probst et al. [1]. However, the shape of the curve is similar for all three theories.

Since germane is a stable molecule, it has been more widely studied than other germanium hydrides. Fig. 4 shows the ionization cross-section for electron impact on germane. Previous theoretical data are reported by Ali et al. [3], Probst et al. [1] whereas Szmytkowski and Denga [4] have reported estimated values of Ionization cross-sections using a simple regression formula. There is only one experimental data point, at 100 eV, reported by Perrin and Aarts [27] and it has a very high experimental uncertainty of 25%. The present data are in very good agreement with almost all reported data throughout the energy range, except the estimated data of Szmytkowski and Denga [4] which lies considerably higher than the present data above 80 eV. The present results are lower than the experimental value of Perrin and Aarts [27], however they still fall within the specified experimental uncertainty.

Fig. 5 shows our calculations of the total (complete) cross-sections for e-GeH_4 scattering. Our present results update earlier results [15]. Here we have used Zhang model for polarization potential which is better at low energies. Thus we are able to report Q_T at energies below 50 eV, whereas in our earlier paper we limited our data to above 50 eV. The other change is that we have used dynamic variation of parameter Δ through Eq. (6). The present

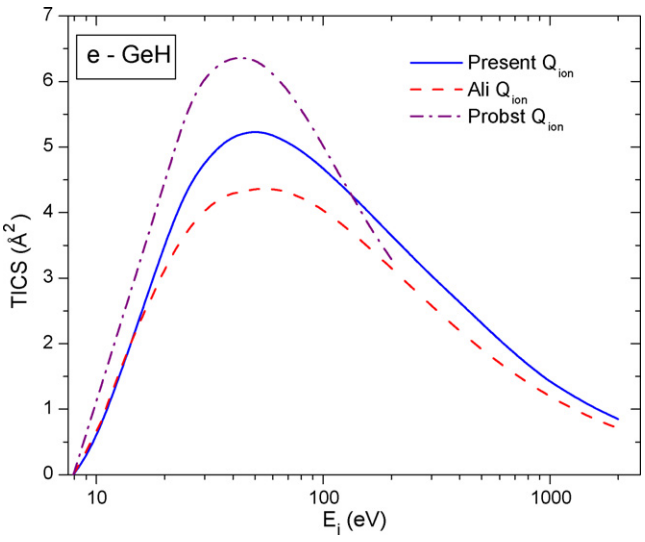

Fig. 1. Total ionization cross-sections for e-GeH scattering. Present total ionization cross-sections (solid line), calculated total ionization cross-sections (dashed line) [3], calculated total ionization cross-sections (dash dot line) [1].

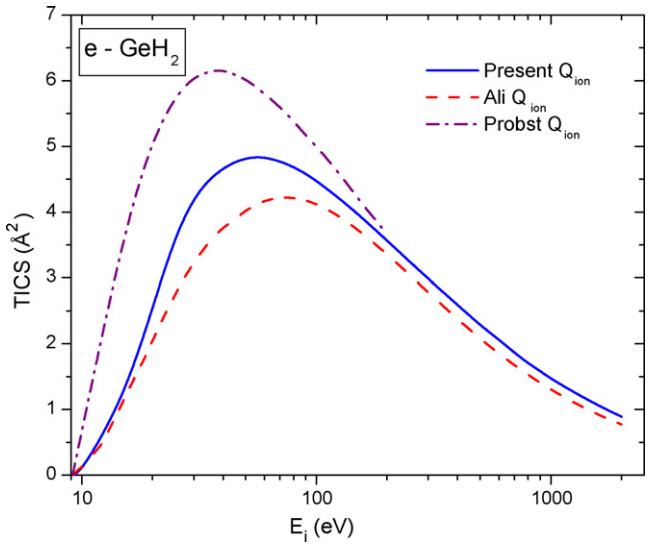

Fig. 2. Total ionization cross-sections for e-GeH_2 scattering. Present total ionization cross-sections (solid line), calculated total ionization cross-sections (dashed line) [3], calculated total ionization cross-sections (dash dot line) [1].

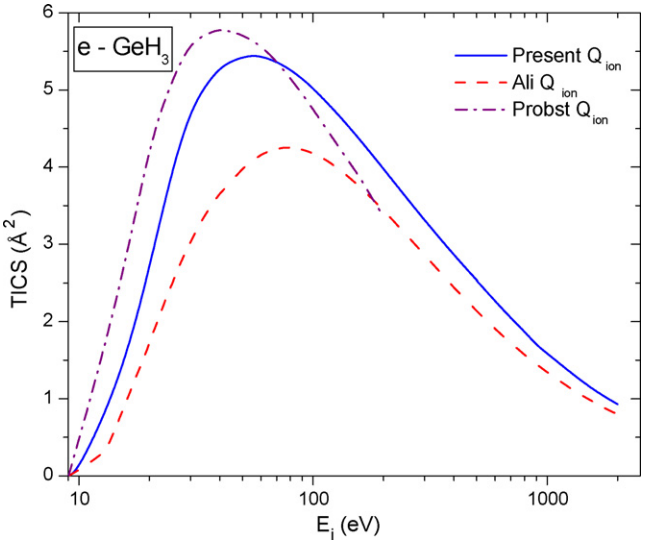

Fig. 3. Total ionization cross-sections for e-GeH_3 scattering. Present total ionization cross-sections (solid line), calculated total ionization cross-sections (dashed line) [3], calculated total ionization cross-sections (dash dot line) [1].

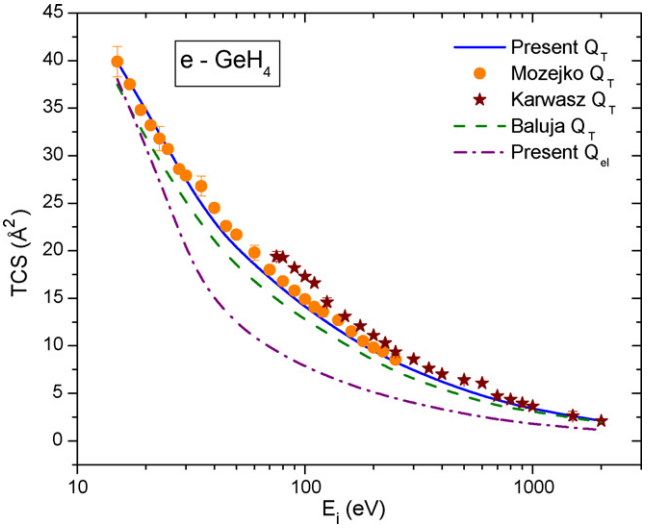

Fig. 5. Total cross-section for e-GeH_4 scattering. Present total cross-sections (solid line), present total elastic cross-sections (dashed dot line), experimental total cross-sections (filled circles) [9], total cross-sections (stars) [10], calculated total cross-sections (dashed line) [8].

results are in excellent agreement with the experimental values of Mozejko et al. [9] across the whole energy range. The experimental results reported by Karwasz [10] are slightly higher than the present values below 200 eV, while above 200 eV they are in very good accord with the present results. The theoretical results of Baluja et al. [8] are slightly lower than the present values. The difference is more at low energies while at high energies present results merge with them. This may be attributed to the difference in the polarization models used, as polarization contribution is more at low energies.

Fig. 6 shows total ionization cross-section of e-Ge_2H_6 scattering. Once again there is scarcity of both theoretical and experimental results with which to compare. The only theoretical results are reported by Ali et al. [3] and the present results are in good agreement throughout the energy range. However the peak in our cross-section lies at slightly higher energy.

Despite the importance of germanium hydrides there is great paucity for both theoretical and experimental data with which to compare the results for all the radicals studied here. Hence in Fig. 7 we have compared mutually our present TCSs values for all the germanium hydrides investigated in this paper. The present study involves, as basic inputs, the atomic charge density, ionization and the polarizability of the target. The size of the molecule is determined by the total number of electrons and their configuration. Q_T increases with increase in the geometrical size and number of electrons of the target.

In Fig. 8, a bar chart shows the relative comparison of the various total cross-sections to the total (complete) cross-sections for e-GeH_4 scattering at 80 eV. It gives the overall picture of all the collision processes involved in the scattering. The total elastic and total inelastic cross-sections are 56.7% and 43.3% of the total cross-section, respectively. The total ionization and total

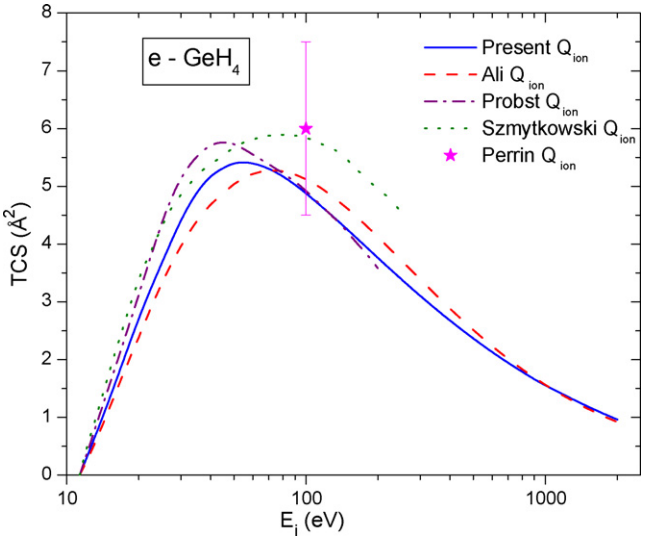

Fig. 4. Total ionization cross-sections for e-GeH_4 scattering. Present total ionization cross-sections (solid line), calculated total ionization cross-sections (dashed line) [3], calculated total ionization cross-sections (dash dot line) [1], estimated total ionization cross-sections [14], experimental total ionization cross-section (star) [23].

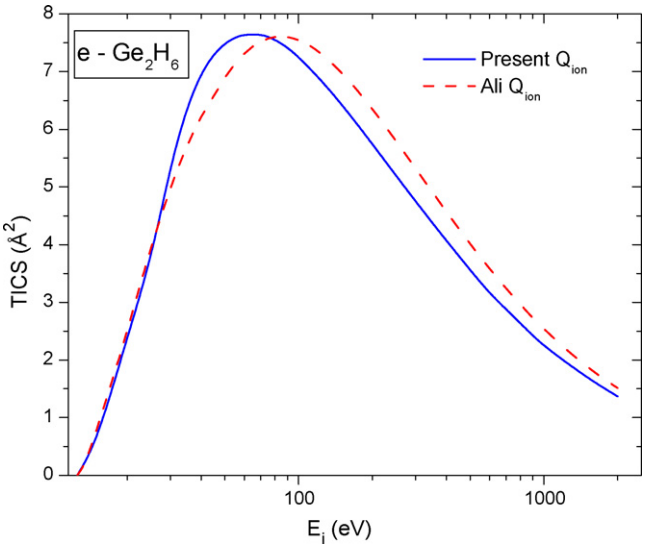

Fig. 6. Total ionization cross-sections for e-Ge_2H_6 scattering. Present total ionization cross-sections (solid line), calculated total ionization cross-sections (dashed line) [3].

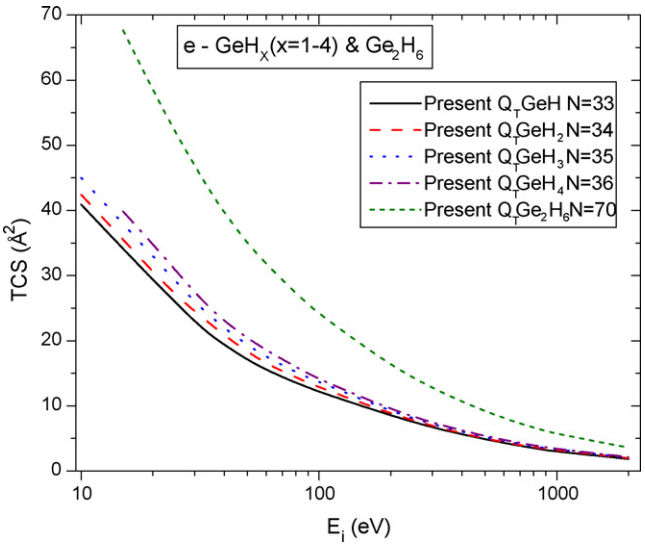

Fig. 7. Comparison of present total cross-sections of different targets (N, number of target electrons). Present total cross-section for GeH (solid line), present total cross-section for GeH_2 (dashed line), present total cross-section for GeH_3 (dotted line), present total cross-section for GeH_4 (dashed dot line), present total cross-section for Ge_2H_6 (short dashed line).

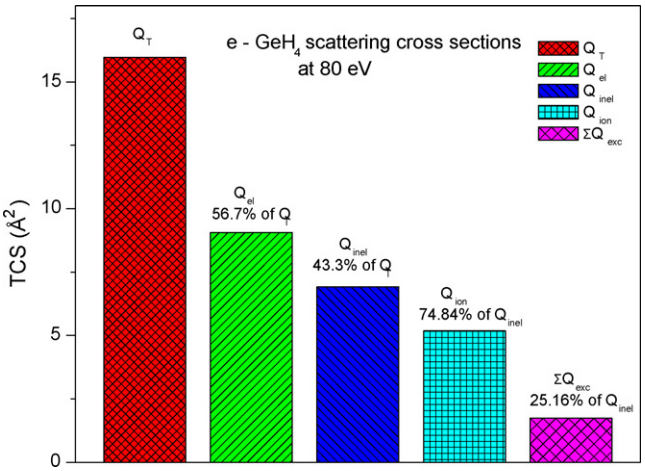

Fig. 8. Relative comparison of various TCSs for e-GeH_4 scattering at 80 eV. Present total cross-section (small crosses), present total elastic cross-section (left slanted lines), present total inelastic cross-section (right slanted lines), present total ionization cross-section (squares), present total excitation cross-section (big crosses).

excitation cross-sections are 74.8% and 25.2% of total inelastic cross-sections.

4. Conclusion

Electron impact total elastic and total inelastic cross-sections have been calculated for the germanium hydrides, GeH_X (X = 1–4) and digermane using the well known spherical complex optical potential method. The total (complete) cross-section serves as an upper limit to all the cross-sections as it includes all the scattering processes. The complex scattering potential-ionization contribution formalism developed by the authors [5,11–17] was used to derive the total ionization cross-section for these targets. This method has been tested successfully for a large number of atomic and molecular targets. The derived theoretical inelastic cross-section serves as the upper limit and gives a useful estimate of the total ionization cross-section. We note that in view of the approximations made here, no definitive values are claimed, but by and large our results fall well within the experimental error limits. It is noted that in Figs. 4 and 6, there is little shift in the peak value. This may be due to other open channels which have not been considered in this paper. The main advantage of the present method is that all the cross-sections (Q_{el}, Q_{inel}, Q_T, Q_{ion}) calculated here are obtained under the same formalism of SCOP. The present theoretical results for the total (complete) and total ionization cross-sections show good agreement with most of other theoretical and experimental investigations. However we hope this work may inspire the experimentalists as there is paucity of experimental data for all germanium hydrides.

Acknowledgements

MVK and CGL thank University Grants Commission New Delhi, for Major Research project under which part of this work is done.

References

[1] M. Probst, H. Deutsch, K. Becker, T.D. Märk, Int. J. Mass Spectrom. 206 (2001) 13.
[2] M.-T. Lee, L.M. Brescansin, L.E. Machado, Phys. Rev. A 59 (2) (1999) 1208.
[3] M.A. Ali, Y.-K. Kim, W. Hwang, N.M. Weinberger, M.E. Rudd, J. Chem. Phys. 106 (23) (1997) 9602.
[4] Cz. Szmytkowski, E.P. Denga, Vacuum 63 (2001) 545.
[5] M. Vinodkumar, C. Limbachiya, B. Antony, K.N. Joshipura, J. Phys. B: Atom. Mol. Opt. Phys. 40 (2007) 3259.
[6] M.A. Dillon, L. Boesten, H. Tanaka, M. Kimura, H. Sato, J. Phys. B: Atom. Mol. Opt. Phys. 26 (1993) 3147.
[7] C. Winstead, P.G. Hipes, M.A.P. Lima, V. McKoy, J. Chem. Phys. 94 (8) (1991) 5455.
[8] K.L. Baluja, A. Jain, V.Di. Martino, F.A. Gianturco, Europhys. Lett. 17 (2) (1992) 139.
[9] P. Mozejko, G. Kasperski, Cz. Szmytkowski, J. Phys. B: Atom. Mol. Opt. Phys. 29 (1996) L571.
[10] G.P. Karwasz, J. Phys. B: Atom. Mol. Opt. Phys. 28 (1995) 1301.
[11] M. Vinodkumar, K.N. Joshipura, C. Limbachiya, N. Mason, Phys. Rev. A 74 (2006) 022721.
[12] M. Vinodkumar, K.N. Joshipura, C.G. Limbachiya, B.K. Antony, Eur. Phys. J. D 37 (2006) 67.
[13] M. Vinodkumar, K.N. Joshipura, N.J. Mason, Acta phys. Slovaka 56 (4) (2006) 521.
[14] P.L. Vieira, F. Blanco, J.C. Oller, A. Munoz, J.M. Perez, M. Vinodkumar, G. Garcia, N.J. Mason, Phys. Rev. A 71 (2005) 032720.
[15] K.N. Joshipura, M. Vinodkumar, C.G. Limbachiya, B.K. Antony, Phys. Rev. A 69 (2004) 022705.
[16] K.N. Joshipura, M. Vinodkumar, B.K. Antony, N.J. Mason, Eur. Phys. J. D 23 (2003) 81.
[17] K.N. Joshipura, B.G. Vaishnav, C.G. Limbachiya, Pramana. J. Phys. 66 (2006) 403; K.N. Joshipura, S. Gangopadhyay, B.G. Vaishnav, J. Phys. B: Atom. Mol. Opt. Phys. 40 (2007) 199.
[18] C.F. Bunge, J.A. Borrientos, At. Data Nucl. Data Tables 53 (1993) 113.
[19] S. Hara, J. Phys. Soc. Jpn. 22 (1967) 710.
[20] X. Zhang, J. Sun, Y. Liu, J. Phys. B 25 (1992) 1893.
[21] G. Staszewska, D.W. Schewenke, D. Thirumalai, D.G. Truhlar, Phys. Rev. A 28 (1983) 2740.
[22] F. Blanco, G. Garcia, Phys. Rev. A 67 (2003) 0022701.
[23] E. Krishnakumar, S.K. Srivastava, J. Phys. B 21 (1988) 1055.
[24] G.P. Karwasz, R.S. Brusa, A. Zecca, Riv. Nuovo Cimento 24 (1) (2001) 1.
[25] R. Basner, M. Schmidt, V. Tarnovsky, K. Becker, H. Deustch, Int. J. Mass Spectrom. Ion Process. 171 (1997) 83.
[26] J.E. Turner, H.G. Paretzke, R.N. Hamm, H.A. Wright, R.H. Richie, Radiat. Res. 92 (1982) 47.
[27] J. Perrin, J.F.M. Aarts, Chem. Phys. 80 (1983) 351.